International Journal of Applied Earth Observation and Geoinformation 144 (2025) 104880

Contents lists available at ScienceDirect

International Journal of Applied Earth Observation and Geoinformation

journal homepage: www.elsevier.com/locate/jag

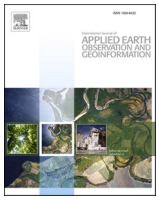

Can optical water types be used as ecological indicators? Insights from a temperate estuary

Giulia Sent [a,*], Evangelos Spyrakos [b], Thomas Jackson [c], Elizabeth C. Atwood [d], Vanda Brotas [a,e], Steve Groom [d], Ana C. Brito [a,e]

[a] MARE—Marine and Environmental Science Centre, Faculdade de Ciências, Universidade de Lisboa 1749-016 Lisboa, Portugal
[b] University of Stirling, Earth and Planetary Observation Sciences, Stirling FK9 4LA, UK
[c] EUMETSAT, Eumetsat Allee, 1D-64295 Darmstadt, Germany
[d] Plymouth Marine Laboratory, Prospect Place, PL1 3DH Plymouth, UK
[e] Departamento de Biologia, Faculdade de Ciências, Universidade de Lisboa 1749-016 Lisboa, Portugal

ARTICLE INFO

Keywords:
Remote sensing
Transitional waters
Water quality
Classification
Ecological indicators
Monitoring
Estuaries

ABSTRACT

Monitoring water quality and understanding how estuarine ecosystems respond to environmental changes is essential to sustain their ecological integrity and associated ecosystem services. In this study, we demonstrate that Optical Water Type (OWT) classification from Sentinel-2 MSI can be used as a stand-alone product rather than an intermediate tool for algorithm refinement, providing valuable insights for environmental monitoring, using the Tagus Estuary as an example. In-situ measurements (Chl-*a*, temperature, salinity, pH, and dissolved oxygen) were employed to characterize environmental conditions associated with OWT classes and to analyse the spatio-temporal and tidal variability during 2017–2024. We identified distinct water quality profiles among groups of OWTs, which were associated with marine, transitional and riverine waters with different physico-chemical characteristics that were related to different environmental drivers. Tides significantly influenced the distribution of OWTs, with high and neap tides favouring the occurrence of clearer marine waters. Specific OWT classes emerged as indicators for key environmental processes, including marine water intrusion, freshwater inputs and phytoplankton-rich waters. Time-series analysis revealed a trend of increasing marine waters inside the estuary alongside interannual variability driven by hydro-climatic forcings. Our findings highlight OWT classification as a valuable stand-alone satellite product for water quality monitoring, providing a powerful and scalable tool for estuarine science, policy, and management.

1. Introduction

Estuaries, located at the interface between rivers and oceans, are among the most urbanized yet vital ecosystems on Earth. Their brackish waters and intertidal areas support rich biodiversity, serve as buffers for the discharge of nutrients and pollutants into coastal areas, and provide valuable ecosystem services (Barbier et al., 2011). Given the increasing anthropogenic pressures, understanding natural variability of estuaries is essential to effectively monitor human impacts and support informed water management. For water quality monitoring, environmental agencies typically rely on discrete in-situ sampling, which provide accurate but spatially and temporally limited information. Given the rapid temporal changes and strong spatial gradients in estuarine systems, monitoring approaches require adequate resolution. Satellite remote sensing overcomes these limitations, offering a synoptic view of these dynamic ecosystems. Satellite-based optical methods can measure variations in near-surface water colour, quantitatively expressed as spectral remote sensing reflectance (Rrs^{λ}). These variations are caused by interactions between the incident light and optically-active components such as Chlorophyll-*a* (Chl-*a*), Suspended Particulate Matter (SPM), and Coloured Dissolved Organic Matter (CDOM). While traditional applications focus on retrieving these individual parameters (Werdell et al., 2018; Adjovu et al., 2023), other approaches classify pixels with similar spectral signatures, or Optical Water Types (OWT), allowing delineation of distinct water masses (Devred et al., 2007). OWT classification has been extensively applied to map optical diversity and biogeochemical

* Corresponding author.
E-mail addresses: gsent@ciencias.ulisboa.pt (G. Sent), evangelos.spyrakos@stir.ac.uk (E. Spyrakos), thomas.jackson@eumetsat.int (T. Jackson), liat@pml.ac.uk (E.C. Atwood), vbrotas@ciencias.ulisboa.pt (V. Brotas), SBG@pml.ac.uk (S. Groom), acbrito@ciencias.ulisboa.pt (A.C. Brito).

https://doi.org/10.1016/j.jag.2025.104880
Received 9 July 2025; Received in revised form 9 September 2025; Accepted 24 September 2025
Available online 28 September 2025

variability in open ocean and large lakes (e.g., Moore et al. 2014; Jackson et al., 2017; Spyrakos et al. 2018; Wei et al., 2022; Bi and Hieronymi, 2024; Eleveld et al., 2017). However, its use in more complex environments, like estuaries, has been focused primarily on refining algorithms for retrieving water quality parameters (Sun et al., 2014; Uudeberg et al., 2020; Yue et al., 2020). This often overlooks the ecological context that is necessary for a comprehensive understanding of biogeochemical variability. Inherently, OWT classes reflect distinct optical (and potentially ecological) conditions (Platt and Sathyendranath, 1999), thus making them a promising stand-alone satellite product. This direct application, however, remains largely unexplored in estuarine research, where linking OWTs to ecological meaning could greatly enhance our monitoring capabilities. Furthermore, the existing applications of OWT to estuarine systems limit their focus on algorithm refinement and describing spatio-temporal patterns rather than investigating how optical variability responds to environmental drivers.

This work aims to assess the OWT classification as an independent satellite product, applicable in multiple interdisciplinary contexts within estuarine sciences, policy and water management. Here, we evaluate an OWT classification from Sentinel-2 imagery to enhance our understanding of estuarine dynamics and forcing mechanisms. The Tagus estuary serves as an ideal testing location, given its complex hydrodynamics, pronounced marine-to-riverine gradients, and well documented long-term environmental changes. Specifically, we: i) characterize OWTs by linking the satellite-derived classes with in-situ measured biogeophysical variables; ii) investigate relationships between OWT occurrences and key environmental forcing (tides, river discharge, wind stress, air temperature); and iii) identify specific OWT classes as proxies for critical environmental processes. Furthermore, the potential of this methodology is showcased through time-series analysis of OWT frequency for the period 2017–2024. The known limitations and other potential applications of this approach in interdisciplinary research and in support of water management policies are also discussed.

2. Data and methods

2.1. Study area

The Tagus estuary (Fig. 1), located in the western Iberian Peninsula, is one of the largest and most significant wetlands in Europe, covering an area of 320 km^2 with a mean volume of 1.9 km^3 (APA, 2016). It forms a transitional system extending ~30 km inland from the Atlantic Ocean to the Tagus River, and is characterized by strong marine-to-riverine gradients (Vale and Sundby, 1987; Rodrigues et al., 2020; De Pablo et al., 2022). Morphologically, it can be divided into three regions (Neves, 2010; Vaz and Dias, 2014; De Pablo et al., 2022): i) the upstream region, where the Tagus enters the estuary (average depth of ~2 m); ii) the middle basin, the widest estuary area (15 km wide, average depth of ~ 7m) which includes two southern bays with intertidal flats and long residence times; and iii) the downstream region, a deep (40 m maximum) long and narrow channel that connects the Atlantic Ocean to the main estuary. In this work, the three regions will be referred to as "inn" (inner), "mid" (middle) and "out" (outer).

Water circulation is driven predominantly by semidiurnal tides, with additional influence from river discharge, wind, and storm surges (Neves, 2010). Tidal amplitude averages 2.4 m at the inlet, varying from 0.9 (neap tide) to 4.1 m (spring tide). The estuary is well-mixed predominantly and Ebb-dominated due to its extensive tidal flats (20–40 % of the estuary) (Fortunato et al., 1999). Freshwater input, mainly from the Tagus (annual mean discharge: 263 m^3/s), varies significantly both seasonally and interannually, and can affect circulation and stratification processes.

2.2. Description of optical water types cluster set

The OWT classification methodology developed by Atwood et al. (2024) was used in this study. This pan-regional OWT library consists of 17 classes generated through fuzzy c-means clustering of Sentinel-2 MSI

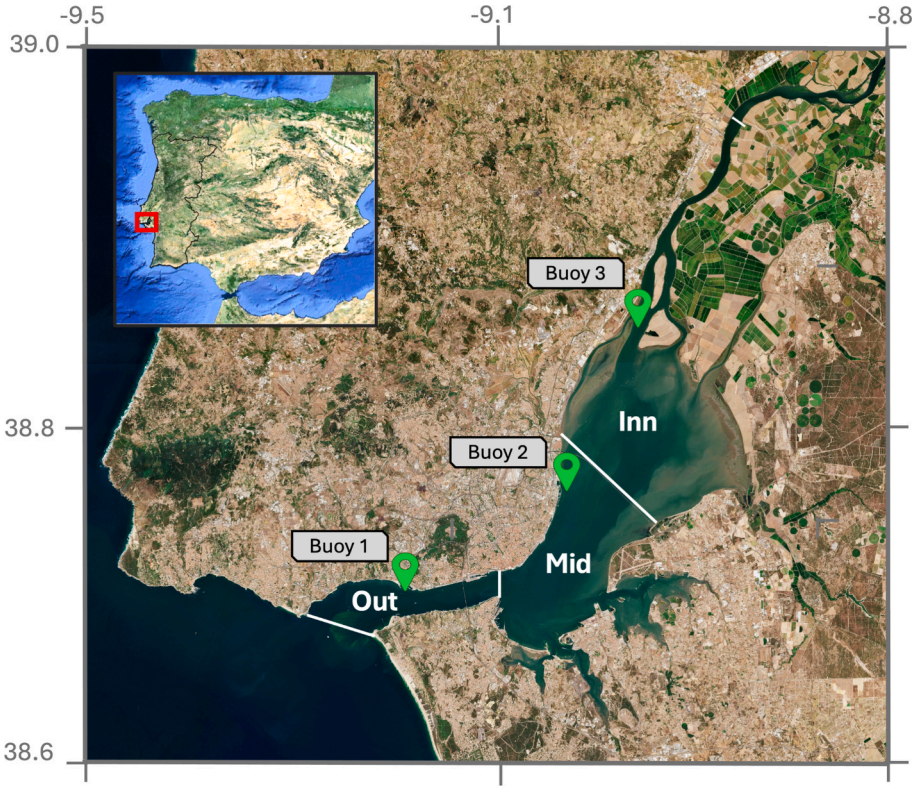

Fig. 1. The Tagus estuary with the location of the three CoastNet buoys (https://coastnet.pt) measuring continuous water quality data and the regions (inn, mid, out) used herein.

Rrs spectra collected from 6 transitional aquatic systems across Europe. The Tagus estuary was included in the training dataset, supporting the applicability of these classes to our study area. A detailed description of the methodology used to obtain the cluster set can be found in Atwood et al. (2024). The Sentinel-2 satellites were selected because of the fine spatial resolution of the onboard MultiSpectral Instrument (MSI) (10, 20, 60 m depending on the band), suitable for observing the narrow areas and sharp gradients typical of estuarine environments.

2.3. Sentinel-2 processing and classification

Sentinel-2 Level-1C data over 2017–2024 were atmospherically corrected and quality checked through the Calimnos processing chain (Stelzer et al., 2020). The processor uses Polymer Atmospheric Correction (AC, v4.15, (Steinmetz et al., 2011)) and a set of quality flags from both the AC processor (out of bounds, bright pixels masks) and IDEPIX (invalid, clouds, cirrus, land masks) (Wevers et al., 2021). The image processing chain follows Atwood et al. (2024), to ensure methodological consistency with the OWT dataset derivation. The Polymer AC was selected by Atwood et al. (2024) for its higher performance in complex waters.

The derived water-leaving reflectances were log-transformed and a membership score was computed using the constrained Euclidean distance. The dominant OWT was defined as the class with the highest membership value. A mask representing the intertidal area and sandbanks in shallow waters was applied to all imagery to remove areas with possible bottom reflection. The Sentinel-2 images were further grouped into eight tidal phases according to the method proposed in Sent et al. (2025), accounting for semidiurnal and fortnightly cycles. Due to the fixed satellite overpass time (~11:30 UTC ± 8 min) the dataset is biased towards certain tidal conditions, with early ebb phases being underrepresented (see section 2.5.1).

2.4. Environmental data

Water quality data from in-situ sensors were used to define the environmental characteristics associated with the OWT classes by pairing concurrent in-situ and satellite OWT observations (match-ups). Environmental and hydrological parameters were used to investigate the potential relationship between OWT variability and specific environmental drivers. A comprehensive literature review (e.g., Gameiro et al., 2007; Neves, 2010; Vaz and Dias, 2014; De Pablo et al., 2022; Cereja et al., 2022), identified three key environmental factors influencing the Tagus estuary's hydrological and ecological dynamics, namely: i) tides, ii) river discharge and iii) wind stress. Air temperature was also used as an indicator of seasonal variability.

2.4.1. Water quality observations from in-situ sensors

In-situ data were obtained from the Portuguese Coastal and Monitoring Network (CoastNet; https://coastnet.pt) for three YSI/EXO2 multiparametric sensors deployed along the ocean-to-river gradient inside the Tagus estuary (Fig. 1). The dataset includes Temperature (°C), Salinity, pH, Dissolved Oxygen (%sat and μgL^{-1}) and Chlorophyll from fluorometric sensors expressed as concentration (mgL^{-1}). It should be noted that the fluorometric data represent relative changes in Chl-*a* rather than absolute concentrations. Nonetheless, due to regular sensor maintenance and calibration, as well as demonstrated consistency with historical spatio-temporal trends in the Tagus estuary (Gameiro and Brotas, 2010), these data are considered suitable for analysing relative changes among the different OWT and over time. Measurements were obtained at ~0.5 m depth with 15 min frequency from October 2019 to December 2023, with some temporal gaps due to instruments calibration.

2.4.2. Tides

Tidal data were obtained from the tidal prediction model of Antunes (2007) for the port of Lisbon (https://webpages.ciencias.ulisboa.pt/~cmantunes/hidrografia/hidro_mares.html). Fig. 2 shows the tidal classification method proposed in Sent et al. (2025) and applied to the Sentinel-2 dataset.

As described in Eleveld et al. (2014) and Sent et al. (2025), measurements at a fixed time of day (e.g. the Sentinel-2 overpass) will not capture all possible combinations of semidiurnal and fortnightly phases. For the Tagus estuary, the most observed tidal condition at the time of Sentinel-2 overpass is low tide followed by F1, F2 and F3 (Fig. 2b). E1 and E2 are the least represented tidal phases. Notably, tidal phases are observed at different tidal amplitudes and significant water quality differences can be observed at different tidal conditions (Sent et al., 2025; Cereja et al., 2022).

2.4.3. River discharge, wind stress and air temperature

Tagus river discharge, wind speed and direction, and air temperature data were obtained from the SNIRH database (Sistema Nacional de Informação de Recursos Hidricos). Data covered the same period (Jan 2017–Dec 2024) as the Sentinel-2 dataset. For river discharge, daily mean flow rate and 3-day rolling mean from Almourol hydrological Station (120 km upstream) were used.

Hourly wind data and air temperature were obtained from the Monte de Caparica meteorological station. The zonal (*u*) and meridional (*v*) wind components were calculated, where positive u indicates westerly winds and positive v indicates southerly winds. Daily mean values of these components were used in the analysis. Regarding air temperature, the 8-day rolling mean previous to the satellite overpass date was used.

2.5. Match-up criteria

Match-up analyses were performed to describe the ecological profile of each OWT. A match-up was considered when at least 5 of the 9 satellite pixels within a 3x3 box (resampled to 60 m resolution) centred on the buoy location were valid (see Section 2.3), and the average of the three in-situ observations centred around 11:30 UTC (± 8 min from Sentinel-2 overpass) was used for each buoy. Each variable was tested for statistically-significant differences among the different OWTs using the non-parametric Kruskal Wallis test (scipy.stats.kruskal from python package *SciPy* v1.14.0, Virtanen et al., 2020), as all parameters showed a non-normal distribution (tested with Shapiro-Wilk test through the scipy.stats.shapiro module from Python package *SciPy* v1.14.0).

2.6. Framework to relate environmental forcing to OWT changes

To assess OWT dynamics and to understand the influence of different environmental drivers (see Section 2.4), two complementary approaches were employed: 1) comparison of the dominant OWT under different tidal regimes; 2) Principal Component Analysis (PCA) applied to a fixed tidal condition to assess the influence of secondary environmental drivers under minimal tidal influence. Neap high tide was selected as it is the condition with lowest tidal currents (Vale and Sundby, 1987) and, therefore, the preferred one to see the effects of the smaller scale drivers. Neap high tide is also the tidal phase sampled by traditional in-situ monitoring programs.

The methodological approach is schematized in Fig. 3.

3. Results

3.1. Overview of the OWT dataset

Fig. 4 shows the mean spectra of the 17 OWT classes (Fig. 4a) and the spectral differences among OWTs expressed as z-score (calculated through the scipy.stats.zscore from python package *SciPy* v1.14.0, Virtanen et al., 2020) normalized reflectance (Fig. 4b). Spectral similarities among classes, along with the analysis of the geographical occurrence of the dominant OWTs in the Tagus estuary (Fig. 1 in S.M.), informed an

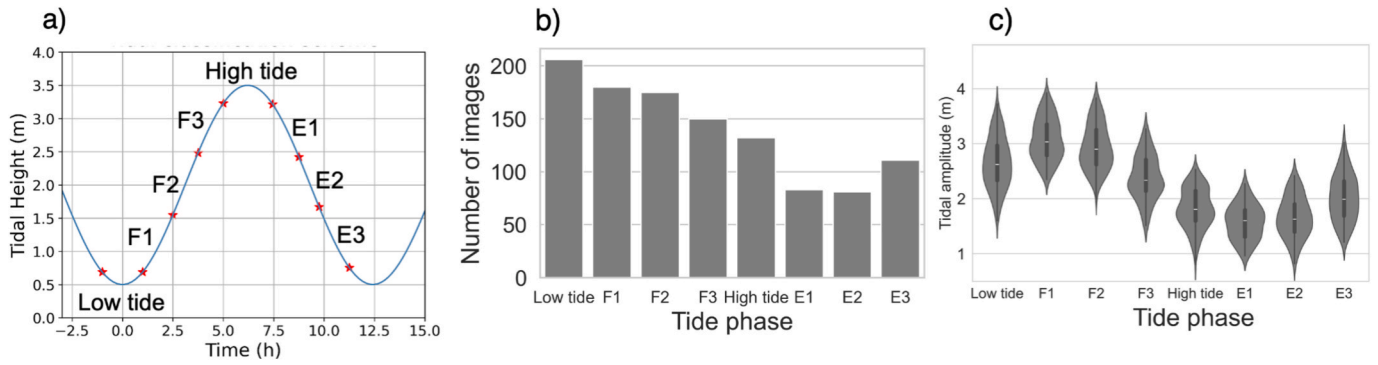

Fig. 2. a) Tidal classification used to group S2-MSI images per tidal phase. b) Distribution of S2-MSI images per tidal stage, and c) tidal amplitude observed for each of the 8 tidal stages.

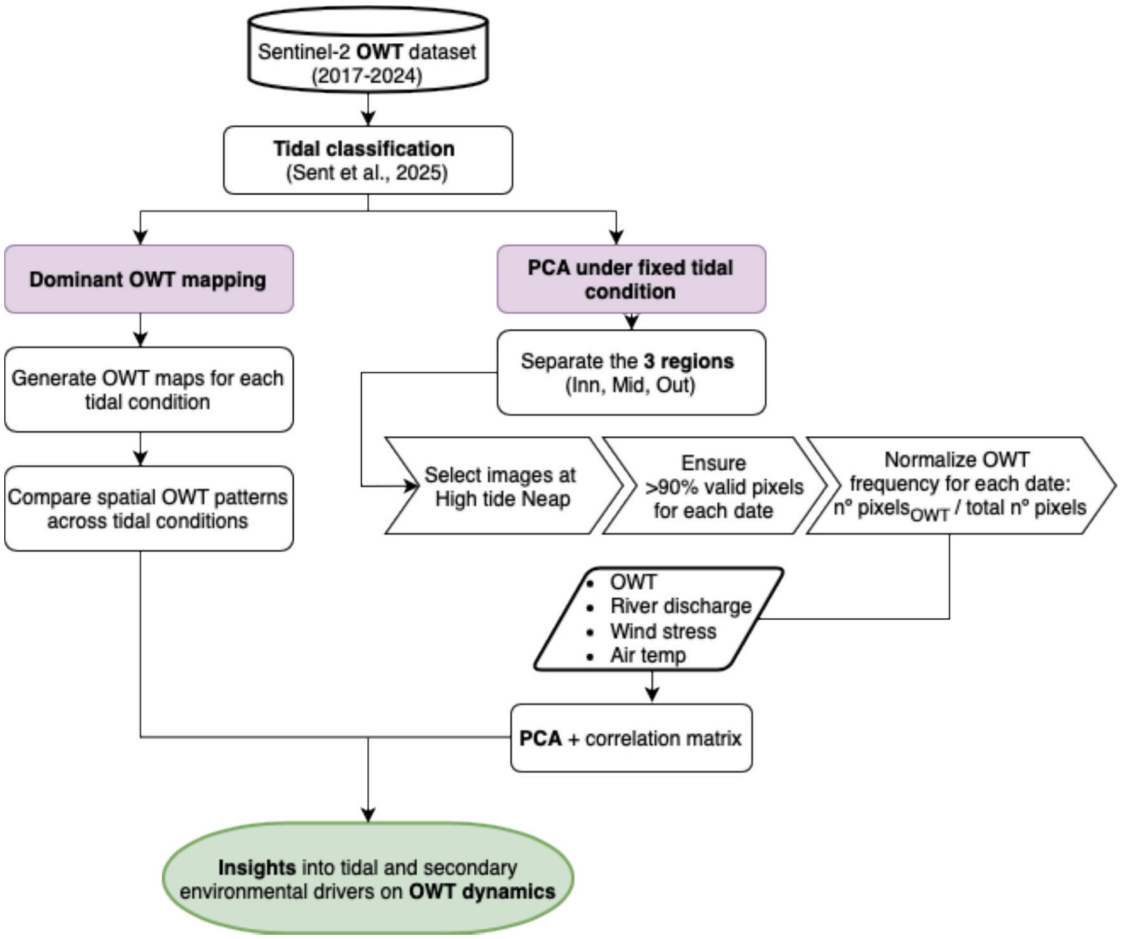

Fig. 3. Flowchart of the methodological approach used to assess the influence of different environmental drivers on OWT dynamics in the Tagus estuary.

initial grouping of the OWT classes into three broader categories (see details below): marine (OWTs 1, 2, 3, 4, 5, 6, 7, 9), transitional (OWTs 8, 10, 12, 14, 16) and riverine (OWTs 11, 13, 15, 17). This preliminary grouping served as a framework for the main analysis of this study and is intended for regional use, as labels reflects the geographical occurrence of OWTs in the Tagus estuary.

Marine OWTs, occurring mainly outside and at the estuary's outer region (Fig. 1 in S.M.), are characterized by higher reflectance in blue and green bands, typical of clear oceanic waters. Among these, OWT 1, 3, and 7 present distinct spectral shapes marked by lower reflectance at 443 nm, corresponding to the primary absorption peak of Chl-*a*, and higher reflectance at 665 and 705 nm – commonly associated to higher scattering from particles. These features suggest that these specific classes may represent higher phytoplankton biomass.

Transitional OWTs mostly occupy the main estuary basin. They show a pronounced reflectance peak at 560 nm, with reflectance decreasing toward the blue region and increasing towards the red (Fig. 4b). The enhanced light absorption in the blue region suggests higher phytoplankton and/or CDOM concentrations. Concurrently, the higher reflectance in the red region of the spectra (665 and 705 nm), indicates increasing turbidity levels with increasing OWT class index.

Riverine OWTs occurring mainly in the upstream region of the estuary, present the most pronounced spectral shift, with strong absorption in the blue wavelengths, and a distinct high reflectance peak at 705

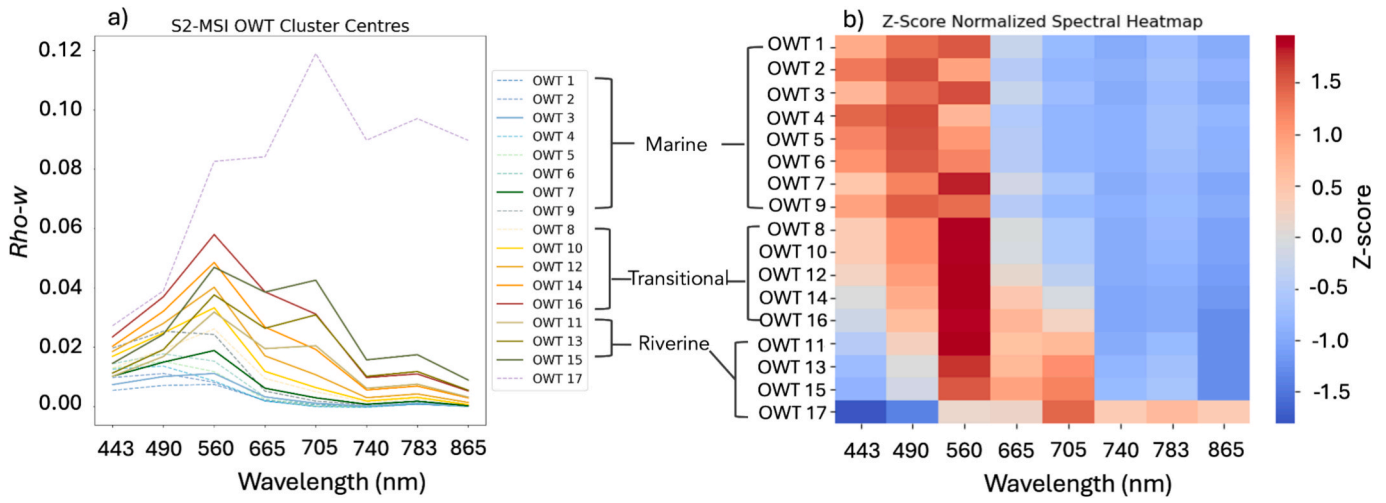

Fig. 4. a) Optical Water Types (OWT) cluster centres from Atwood et al. (2024); the most representative classes within the Tagus are shown with solid lines. b) Shape differences across OWT classes expressed as Z-Score. Marine, transitional and riverine groups were identified in the present study. OWTs are ordered by group rather than numerical index.

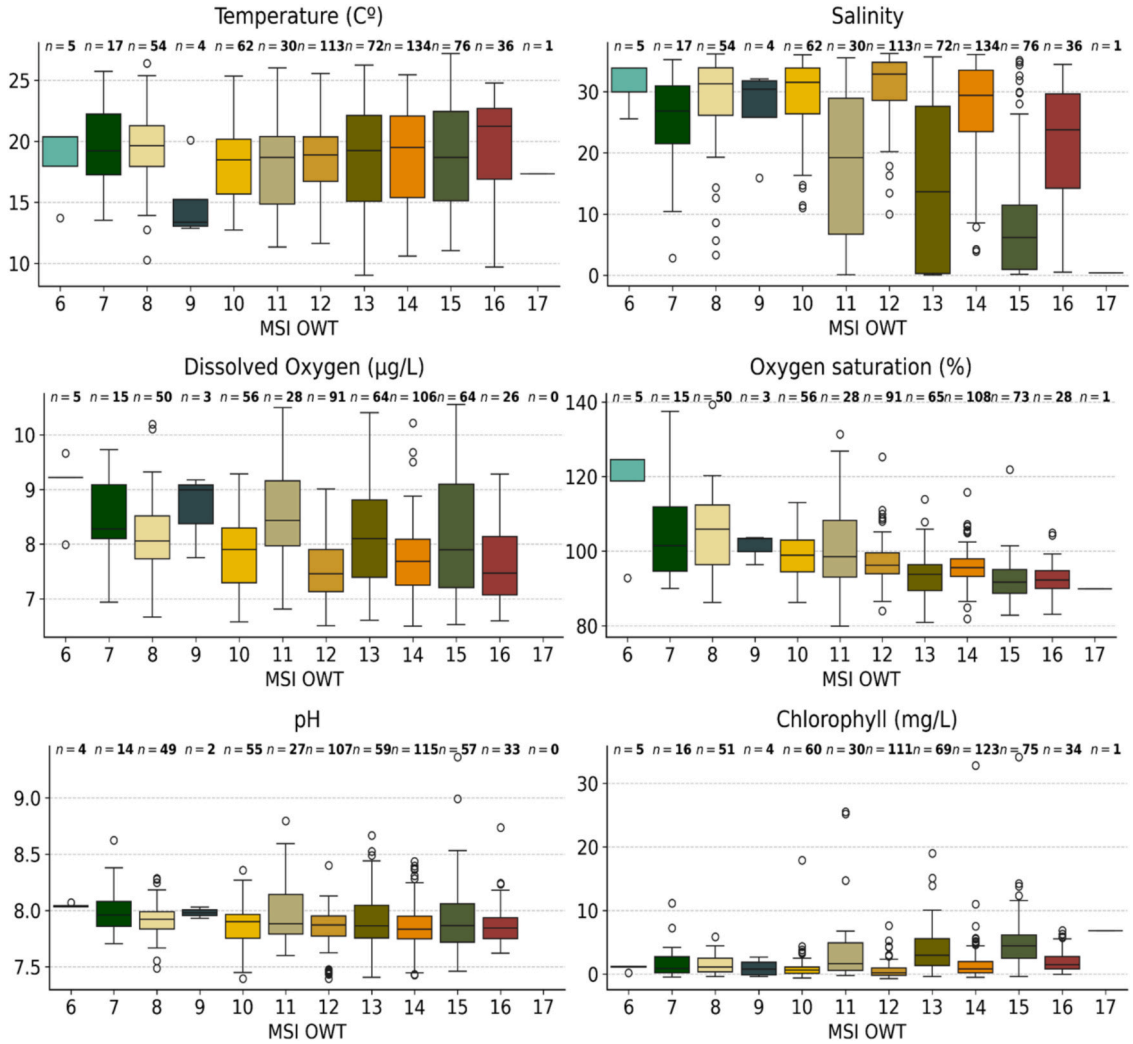

Fig. 5. OWT characterization with in-situ data (Temperature (°C), Salinity, Dissolved Oxygen (µg/L), Oxygen saturation (%), pH, Chlorophyll (mg/L)) from the three CoastNet buoys. In each boxplot, the percentiles (25th, 50th and 75th) are shown as horizontal lines. The number of data points per OWT is indicated on top of each corresponding box.

nm. These characteristics are consistent with high concentration of CDOM and/or phytoplankton and suspended sediments, all established characteristics of riverine waters.

3.2. OWT characterization with in-situ data

The characterization of individual OWTs with concurrent in-situ data is shown in Fig. 5.

All in-situ parameters demonstrated statistically-significant differences among OWT classes ($p < 0.05$), except for temperature ($p = 0.22$). It is important to note that the in-situ dataset does not uniformly represent all OWTs, with OWTs 10, 12, and 14 being the most frequently sampled and most of the marine classes (1, 2, 3, 4 and 5) absent in the dataset (Fig. 5). Considering that our multi-year in-situ dataset provide a comprehensive coverage of hydrological and seasonal conditions, the absence of marine classes reflects their actual absence in the Tagus estuary rather than a sampling gap. The ecological characterization, as described below, confirms the preliminary grouping of OWT classes into three distinct water masses origin (marine, transitional, and riverine), with few exceptions.

The available marine group with in-situ data (OWTs 6, 7, 9) is characterized by waters showing high salinity (mean 27.6), higher pH (mean pH 8.01), supersaturated oxygen levels (mean 109 %) and low Chl-*a* (mean 1.34 mg/L). OWT 7 stands out in this group because of its relatively higher Chl-*a* content, increased pH and O_2, and reduced salinity. This OWT presents a distinct spectral shape among the marine classes, with an absorption peak at 443 nm.

Although OWTs 8 and 10 were preliminary identified as transitional waters due to their spectral similarity to OWTs 12, 14 and 16 (Fig. 4b) and their location inside the estuary basin (Fig. 1 in S.M.), they exhibit salinity and oxygen saturation levels typical of marine waters. However, their lower pH, oxygen concentration, and spectral features (Figs. 4b and 5) align them more closely with transitional and riverine waters. This combination, alongside their spatial occurrence, suggests they represent the zone between marine and transitional environments. Transitional OWTs (12, 14, 16) present a pronounced decreasing gradient in salinity, pH, and oxygen saturation, together with increasing Chl-*a* as OWT index increases, although absolute concentrations remain low.

Finally, riverine OWTs (11, 13, 15) present the greatest differences in environmental profiles among all OWTs, mirroring their pronounced spectral differences (Fig. 4b). They show the lowest salinity means (14.08) with minimum values across all data, the highest pH (mean 7.95, max 8.94), the lowest oxygen saturation (mean 96.7 %), and highest Chl-*a* across all classes (mean 4.44 mg/L). Notably, the absolute oxygen concentration is among the highest of all classes, but the saturation is the lowest. This might reflect the lower salinity and cooler temperatures of riverine waters that would permit higher maximum dissolved oxygen potential and, therefore, lower oxygen saturation for a given concentration.

3.3. Environmental factors influencing the presence of OWTs

3.3.1. Tidal variability

Fig. 6 shows the OWT relative frequency for the different tidal conditions at the buoys locations. Relative frequencies are presented to account for the unequal number of Sentinel-2 observations across tidal phases (See Section 2.4.2). Overall, OWT classes 6 to 10 are more frequent at higher tides and neap tides, while classes 13 to 17 are observed more often at lower tides. This is an expected pattern as higher-index OWTs are associated with transitional and riverine waters that we expect to be present at lower tidal conditions. The spatial distribution of the dominant OWTs of different tidal phases is shown in Fig. 7. Different tidal phases are observed under different tidal amplitudes (see Section 2.4.2). Specifically, ebb phases are generally observed during lower tidal amplitudes (neaps), implying weaker tidal currents compared to flood phases. This distinction is reflected in the OWT distribution: ebbs are predominantly characterized by a gradient of OWTs with overall lower index (OWTs 7, 8, 10, and 12) and reduced river plume, while floods exhibit a gradient characterized by overall higher index classes (10, 12,

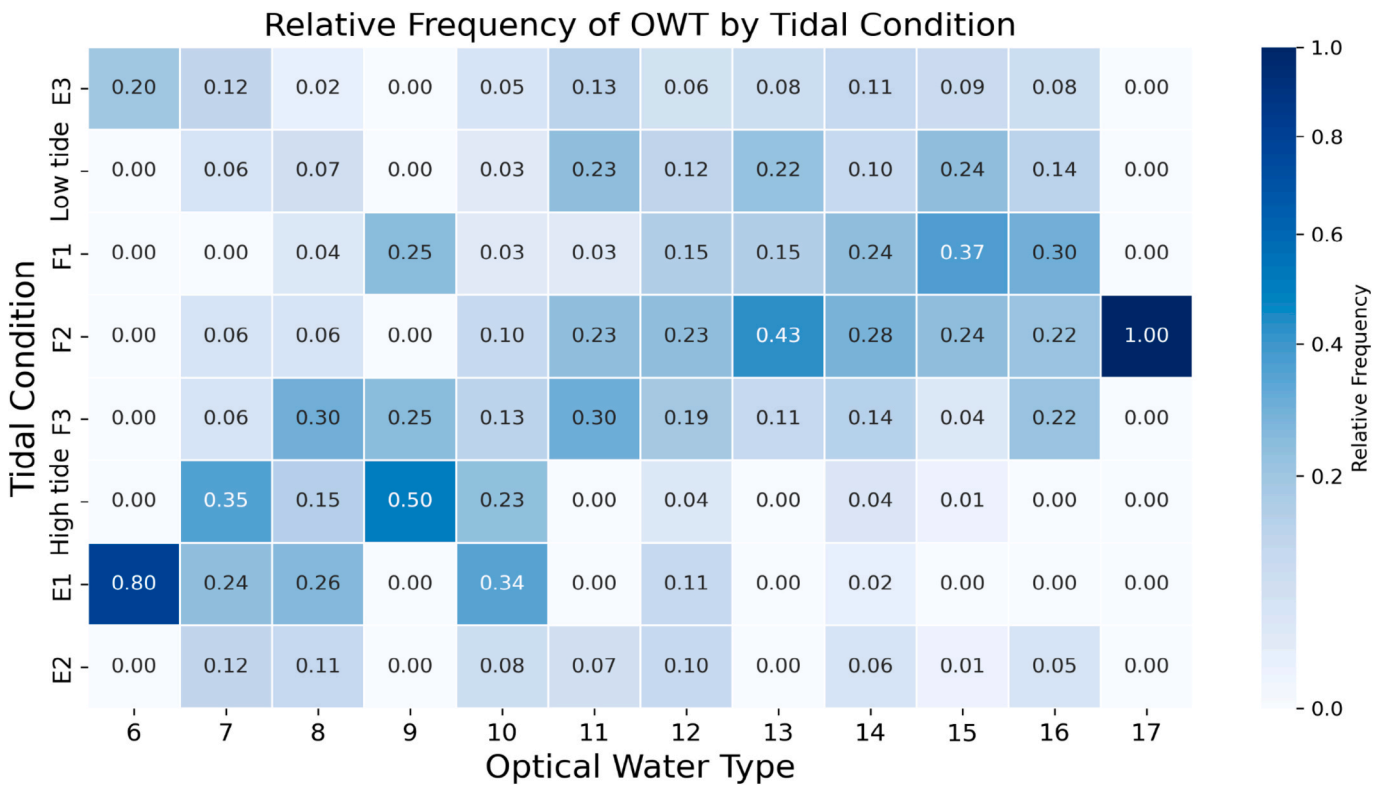

Fig. 6. Relative frequency of OWT by tidal condition at match-up stations.

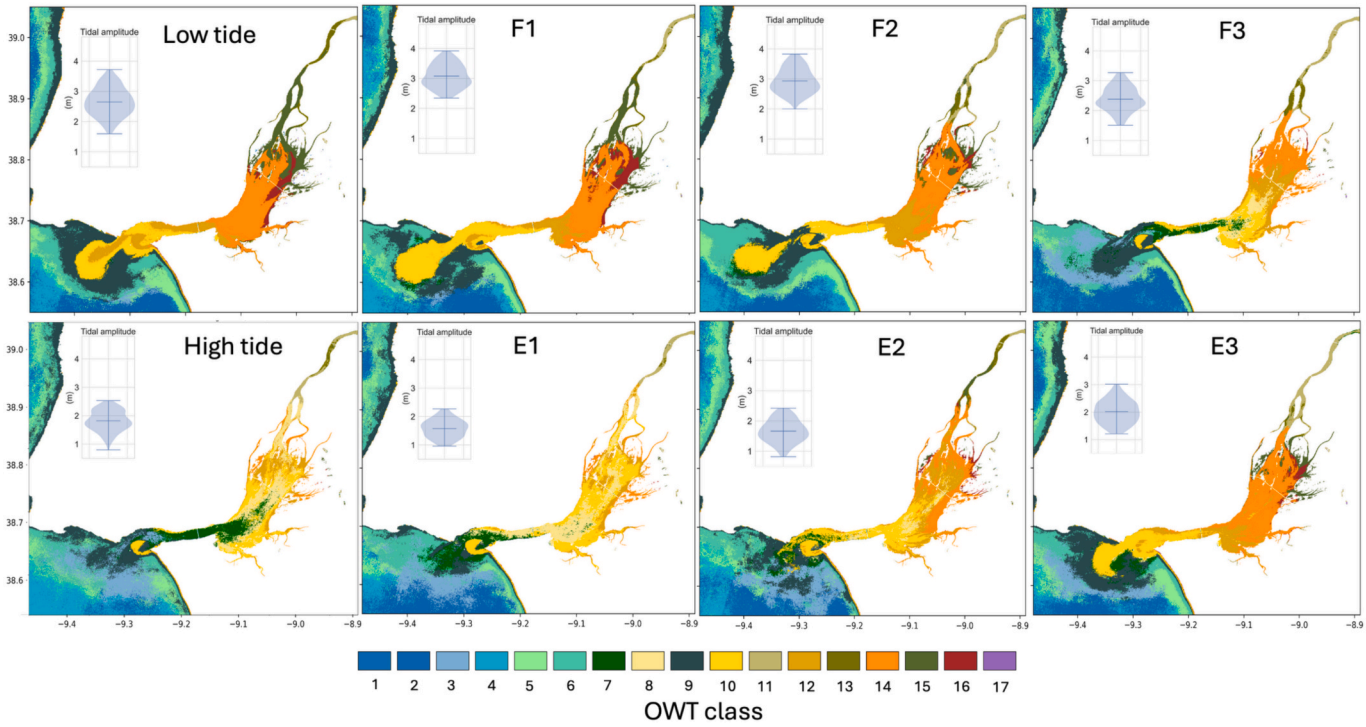

Fig. 7. Spatial distribution of dominant OWTs (OWT 1 to 17) for each tidal phase (F-flooding, E-ebbing) obtained as OWT memberships sum for all available images for each tidal phase. Inset violin plots on each map show the tidal amplitude distribution for the images at each phase.

and 14), indicating that tidal amplitude plays a crucial role in water types distribution.

The upstream parts of the estuary are dominated by the riverine OWTs 11, 13, 15 at all tidal conditions, with more turbid classes (higher index, OWT 15 and 13) dominating during lower tidal conditions and extending downstream. During E2, which is the tidal phase with the strongest tidal currents due to tidal asymmetry (ebbs shorter than floods, Fortunato et al., 1999), the upstream reaches of the "inn" region exhibit turbid riverine waters similar to low tide conditions (OWT 15, 13). In the "mid" and "out" regions, OWT 7 is observed at F3, High tide, E1 and E2, tidal conditions that correspond to high tide and/or neap tides. As described in Sections 3.1 and 3.2, OWT 7 represents marine waters with higher phytoplankton content. Its spatial extent peaks at high tide, dominating the lower area of the "mid" region. It is then flushed out of the estuary during ebbs.

3.3.2. *River discharge, wind and air temperature*

The effect of river discharge, wind and air temperature (season) on OWT variability, was assessed by performing PCA on a fixed tidal condition (neap high tide, more details in Section 2.6), and was further supported by correlation matrices. PCA (Fig. 8) identified covariance (co-occurrence) of OWT classes belonging to the same group, reflecting the previously identified riverine, transitional and marine waters, consistent across the three estuarine regions. In all areas, marine and transitional classes significantly contributed to PC1, showing PC loadings with opposite direction reflecting mutually exclusive conditions.

In the "inn" region (Fig. 8a), PC1 and PC2 explain 44 % of the total variability. PC1 relates mainly to positive u- and v- wind-components, while PC2 to air temperature. Transitional (OWTs 16, 14, 12, 10) and marine (OWTs 3, 7) classes strongly contribute to PC1, in opposite directions, with marine waters favoured by south-westerly winds. Riverine OWTs (11, 13, 15) exhibit strong covariance and correlation with river discharge ($r = 0.9$, 0.4, and 0.4 respectively).

The "mid" region (Fig. 8b) is characterized by overall clearer waters than the "inn" region, yet showing similar patterns regarding environmental forcing. Increased air temperature ($r = 0.5$) and westerly winds ($r = 0.4$) are associated with green marine waters inside the estuary (OWTs 3, 7), contributing to PC1 (23 % of total variability) opposite to transitional classes (OWTs 14, 12, 10). The variability of other marine classes, OWT 5 and 6, along PC2 (19 % of total variability), is partially explained by low river discharge and southerly winds. Despite the expected dilution of riverine and marine waters, OWT 11 (the clearest of the riverine classes) maintains a strong correlation with river discharge ($r = 0.7$).

In the "out" region (Fig. 8c), riverine classes do not occur at high tide, and clearer waters predominate. PC1 and PC2 explain less variability than the other regions (37 %), suggesting influence from additional environmental factors. Again, transitional (OWTs 10, 12) and marine (OWTs 1,3,7) classes are the main contributors to PC1, in opposite directions, with marine classes occurring at higher air temperature ($r = 0.5$). Other marine classes (OWTs 2, 5, 6, 9), on PC2, occur during low river discharge conditions and show a minor correlation with wind patterns, favoured by south-westerly winds.

Table 1 summarises the hydro-ecological characteristics of the OWT classes with paired in-situ water quality data.

3.4. *Relevance for environmental changes monitoring*

Figs. 9 and 10 illustrate the temporal variability in OWT frequency for the three estuarine regions during high and low tide, respectively. Overall, interannual variability was most evident during high tide across all regions and during low tides in the outer estuarine region. These conditions generally favour the dominance of clearer waters.

There was a general decline over time, across all regions and tidal conditions, in frequency of OWTs 16 and 14 (the most turbid of transitional waters) alongside an increase in frequency of OWTs 1, 3 and 7, which are representative of clearer, marine waters (Fig. 2 in S. M.). Notably, this trend is clear for both tidal conditions, while it is more pronounced during high tide in the "inn" and "mid" regions and during low tide in the "out" region. In the downstream area specifically ("out"), the clearer OWT classes (1, 3, 6, 7, 8) increased in frequency, whereas transitional classes (OWTs 10, 12, 14) decreased notably.

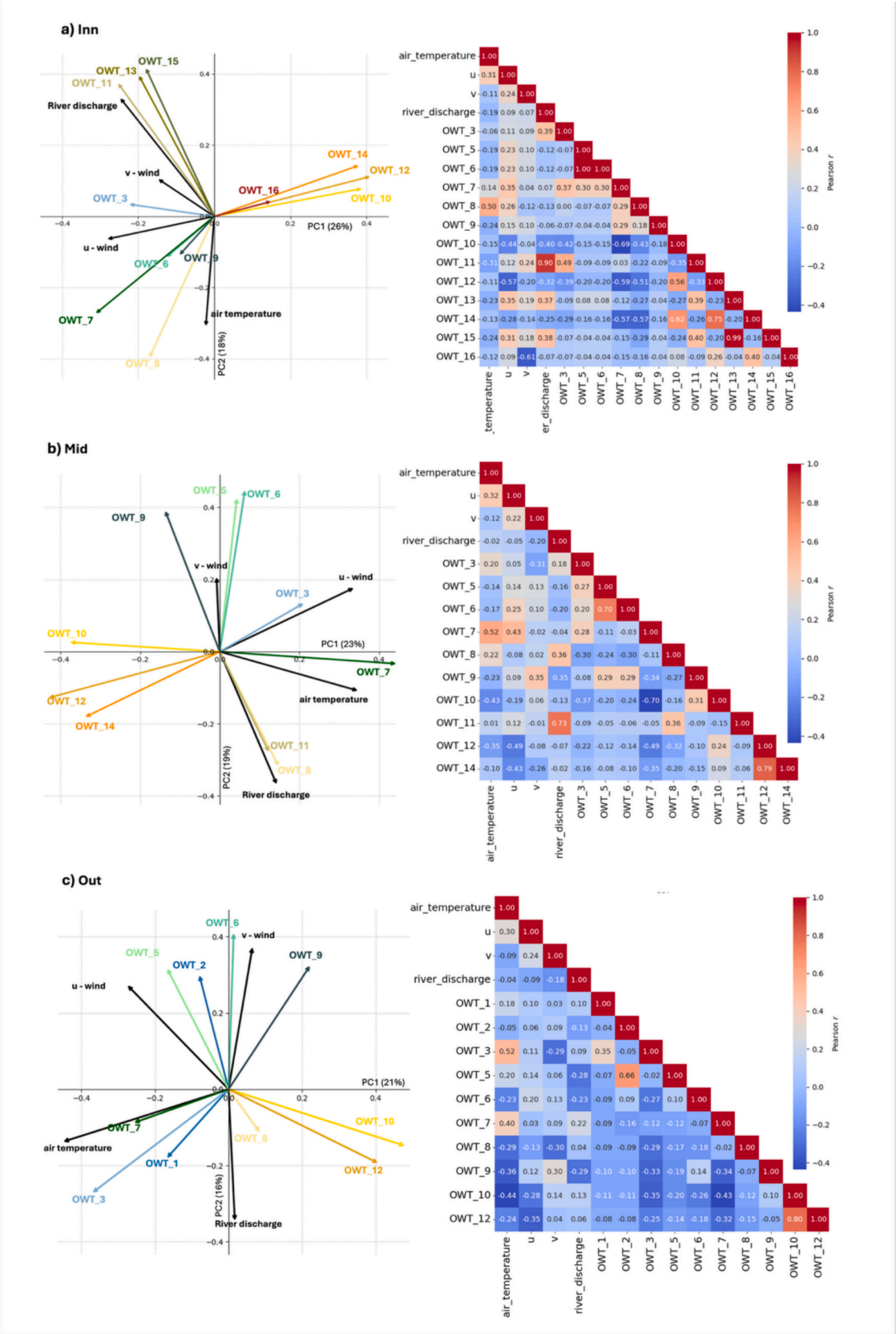

Fig. 8. PCA and correlation matrix (Pearson correlation) of normalized OWT frequency and environmental drivers (river discharge, u-zonal and v-meridional components of the wind, and air temperature) for the three regions of the estuary at high tide.

Table 1
Summary of the hydro-ecological characteristics associated with the different OWT with paired in-situ data in the Tagus estuary.

OWT group	Brief description	Summary of main characteristics
6, 7, 9	Marine waters	Oligo-alkaline, clear waters, with high salinity and supersaturated oxygen levels (>100 %). Mostly found in the downstream region of the estuary. OWT 7 is an indicator of higher phytoplankton biomass and mostly occurs during summer months.
8, 10, 12, 14, 16	Transitional waters	Most common water types at all tidal conditions. Pronounced decreasing gradient in salinity, pH, and oxygen saturation, and increasing Chlorophyll with higher OWT index. Spectral characteristics of sediment-dominated waters with increasing turbidity. OWT 8 and 10 represent the zone between transitional and marine environments exhibiting salinity and oxygen saturation levels similar to marine waters, while pH, absolute oxygen concentration, chlorophyll and spectral signature are similar to transitional waters.
11, 13, 15	Riverine waters	Low salinity, low oxygen saturation (<98 %), low pH and higher Chlorophyll content than any other OWT group. Dominating the upper reaches of the estuary with increased spatial extent after higher river discharge events.

The increase in frequency of OWT 3 and 7 with time is indicative of a stronger presence of marine waters inside the estuary in recent years. The years 2023 and 2024 were characterized by pronounced extremes in water types, reflecting stronger riverine and marine influences alongside a marked reduction in transitional OWTs. Intensified southern winds and prolonged, strong river discharge compared to the preceding 5-year period were observed during 2023 and 2024 (Fig. 9), mirrored by changes in OWTs frequency. The "inn" region displayed an increase in frequency of riverine OWTs (11, 13, 15), at both low and high tide. Transitional OWTs, most notably OWT 16, decreased in frequency, with OWTs 14, 12 and 10 nearly disappearing in the "out" and "mid" regions. Concurrently, there was an increase in frequency of marine waters (OWTs 1, 3, 7) across all regions and tidal conditions.

The extreme and rarely appearing OWT 17 was present in the "inn" region at low tide at the beginning of 2018 and end of 2022, corresponding to the strongest river discharge events recorded during the period under analysis.

4. Discussion

4.1. Hydrological and environmental forcings to OWT variability

Monitoring estuarine ecosystems requires methods capable of capturing their strong spatial gradients and rapid temporal changes. This study demonstrates that a satellite-based Optical Water Type (OWT) approach, when integrated with ecological and environmental information, is a powerful method for tracking water-mass dynamics and to provide insights into linked environmental processes. Among those processes, tides are known to be the primary driver responsible for water circulation and biogeochemical variability in the Tagus estuary (Neves, 2010; Cereja et al., 2022). This was also supported by results herein, which showed distinct OWT patterns across tidal conditions. High tides favoured the occurrence of clearer, marine OWTs, while low tides were dominated by transitional and more turbid OWTs (12, 14, 16). This is consistent with the turbidity gradient described for the Tagus estuary (Vale and Sundby, 1987). Notably, ebb phases exhibited clearer waters than flood phases, likely reflecting lower tidal amplitude during Sentinel-2 overpasses. During lower tidal amplitudes, weaker tidal currents reduce bottom resuspension, resulting in clearer water conditions (Vale and Sundby, 1987; Valente and da Silva, 2009). However, during E2, the tidal phase with the strongest tidal currents, the upstream estuary is dominated by turbid riverine waters (OWTs 13, 15), similar to conditions seen at low tide. This suggests that in this area, the intensified ebb currents caused by tidal asymmetry (ebbs shorter than floods, Fortunato et al., 1999) can overpass the expected relative reduction in tidal currents associated with lower tidal amplitudes.

Moving downstream, the marine OWT 7 is found to have a specific tidal pattern, as it is observed inside the estuary only during the last stage of flooding tide (F3) and high tide, moving outwards with the ebbing phases. OWT 7 emerged as a potential indicator for marine – phytoplankton-rich waters, as it showed supersaturated oxygen levels (>100 %), high Chlorophyll concentrations compared to all other marine OWTs, and the 443 nm absorption peak (Fig. 2b), all traits indicative of phytoplankton-rich waters.

OWTs 3 and 7 were the most frequent marine classes within the estuary bay, serving as indicators of marine waters intrusion into the estuary. Although transitional waters (OWTs 14, 12, 10) typically dominate the main estuary bay, OWTs 3 and 7 replace these classes during summer months, with their frequency positively correlated with air temperature. Riverine OWTs (11, 13, 15) were associated with freshwater inputs and dominated the upstream reaches of the estuary. Their spatial extent was positively correlated with river discharge (Fig. 8), which was also responsible for the extension of riverine waters into the main estuary basin. Their characteristics, including high chlorophyll concentration, low salinity, higher pH, and low oxygen saturation, suggest that respiration processes (likely organic matter decomposition) dominate in these water types. As suspended sediments, inorganic nutrients and organic matter are largely of fluvial origin in the Tagus estuary (De Pablo et al., 2022; Rodrigues et al., 2020; Cereja et al., 2022; Vale and Sundby, 1987) monitoring the spatial extent and temporal variability of these classes offers a valuable proxy for assessing upstream influences on estuarine water quality.

4.2. Ecological significance of OWTs

While the analysis of the temporal trends was not the primary aim of this work, a preliminary assessment of OWT frequency for the period 2017–2024 demonstrated the monitoring value of an OWT classification with linked ecological information. To reduce tidal aliasing effects, the time series was separated by high and low tide. Additionally, the trends were analysed separately for the three estuarine regions to account for spatial variability in OWT dynamics.

Across the full time-series, a general increase in frequency of both marine and riverine OWTs was observed, at both high and low tides. This trend aligns with model predictions of intensified marine intrusion under different scenarios (Rodrigues et al., 2019; Guerreiro et al., 2015), *i.e.* decreased river discharge. These shifts could significantly impact estuarine ecology by altering habitat availability, nutrient dynamics, and biological productivity. Simultaneously, there was a decrease in frequency of transitional waters – notably, OWT 16 is nearly disappearing at high tide in all regions, suggesting a shift from transitional water conditions towards more extreme marine and riverine signals.

Seasonal patterns were evident for the marine OWT 7, being present consistently between May and October in the "mid" and "out" regions at high tide, aligning with the time window of maximum primary productivity in the Tagus estuary (Gameiro et al., 2011). Interannual variability of OWT classes is also visible: 2023 and 2024, showed increased and prolonged discharge events, yet transitional OWTs remained rare, while marine and riverine OWTs increased in dominance. The years 2023 and 2024 were marked by extreme hydroclimatic anomalies at global scale (Esper et al., 2024; Xie et al., 2025): 2023 being the hottest year on record, with extreme precipitation events and strong El Niño (Fowler et al., 2024). In the Tagus estuary, these years exhibited extraordinary hydrological and climate events, marked by significantly high and prolonged river discharge and south-westerly winds in the Tagus estuary. These events were mirrored in the OWT record. Summer 2023 showed the highest frequency of OWTs 3 and 7 across all estuarine

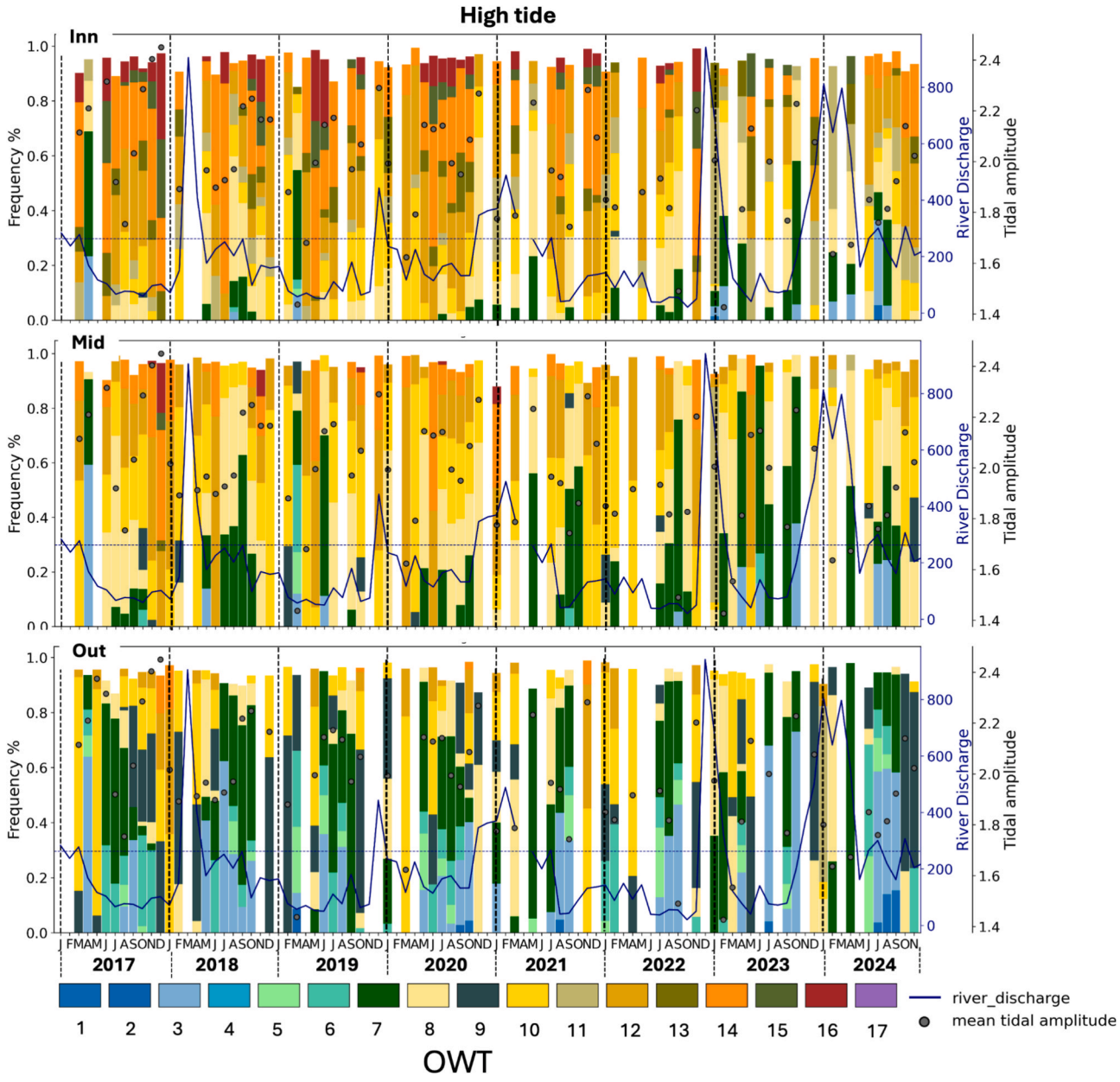

Fig. 9. Monthly time-series of OWT frequency for the three regions of the Tagus estuary for the period 2017–2024 at high tide. River discharge is shown as a solid line and tidal amplitude as a dot.

regions, and unusually clear waters at low tide. These patterns are unique in the 2017–2024 time series and highlight the responsiveness of OWT classifications to detect short-term extreme events, in addition to long-term trends.

4.3. Methodological considerations and known limitations

Mapping the spatio-temporal distribution of OWTs with linked environmental profiles is a valuable approach for understanding and monitoring estuarine systems. However, in complex tidal environments some limitations and methodological considerations must be considered to ensure accurate interpretation.

Sun-synchronous satellites are limited in their ability to observe all possible tidal conditions – in terms of combination of spring-neap and semidiurnal cycles. This is due to fixed overpass times (Eleveld et al., 2014; Sent et al., 2025). As a result, certain tidal phases are over-represented in the satellite record, while others may be entirely missed. This is particularly relevant when training OWT classification models, as the dominant classes may reflect the most frequently sampled conditions rather than the most common ones. Additionally, an optical satellite sensor only observes cloud-free pixels, potentially biasing the observed optical states towards meteorologically calm and stable conditions (Eleveld et al., 2014). Similarly, rare or short-lived events with distinct optical properties (*i.e.*, extreme river discharges, sewage plumes, phytoplankton blooms) may be too infrequent to form distinct clusters and risk being overlooked. This is a common limitation of most of the OWT applications to estuarine research, as most of the studies rely on region-specific libraries (*i.e.*, Uudeberg et al., 2019; Arena et al., 2024; Windle et al., 2025). While effective in defining the most common optical conditions of a system, regional cluster sets risk overlooking ecologically significant short-lived events. Consequently, an extended OWT library containing a wider spectrum of optical states (e.g., Spyrakos et al., 2018; Wei et al., 2022; Bi and Hieronymi, 2024; Atwood et al., 2024) increases the likelihood of detecting rare optical conditions.

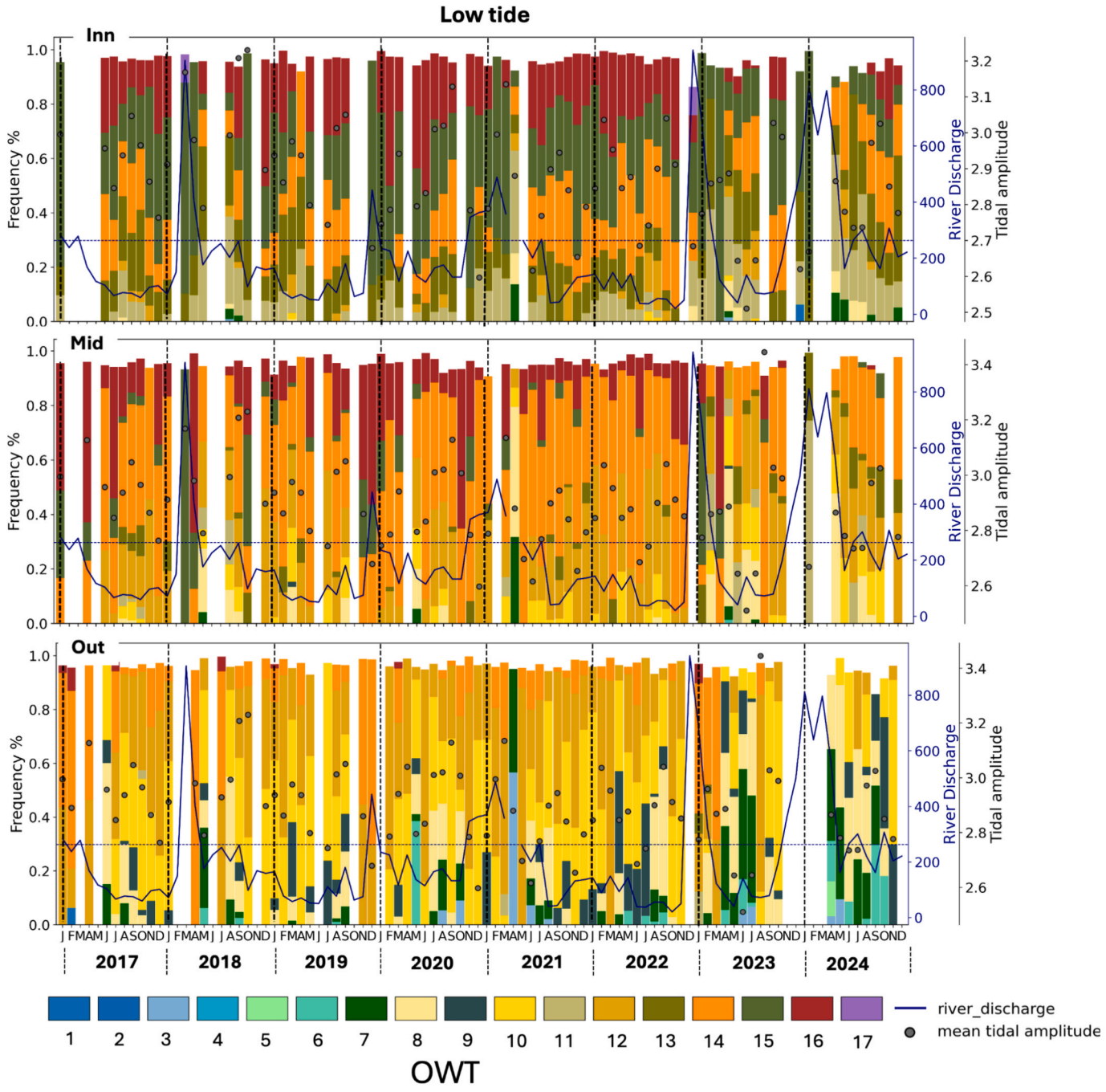

Fig. 10. Monthly time-series of OWT frequency for the three regions of the Tagus estuary for the period 2017–2024 at low tide. River discharge is shown as a solid line and tidal amplitude as a dot.

This work used a pan-regional OWT set (Atwood et al., 2024) with an extended range of optical conditions that enabled the detection of extreme events. While only a subset of the 17 classes regularly occurred in the Tagus estuary, the extreme OWT 17 was identified twice in our 8-year time series (Fig. 9), both following major river discharge events. This class was absent from regional Tagus-specific OWT classifications described in Atwood et al. (2024), therefore, it would not have been identified with a purely regional approach. In addition to the use of a broad OWT dataset, the detection of low membership pixels could be used as a flag for optical – and potentially ecological – anomalies, as low membership values indicate low similarity to any of the reference spectra.

The transferability of the ecological meaning of the OWTs to other estuarine systems is also a key question, as the same OWT might have different biogeochemical characterization in different areas, especially regarding the non-optical components that do not directly influence the spectral signature. The shape and magnitude of *Rrs* spectra are also influenced by the atmospheric correction method, which may introduce specific artefacts and limit the applicability of satellite-derived OWTs to different AC approaches.

4.4. *Further potential applications*

The framework proposed in this study provides a scalable tool for monitoring estuarine systems with broad interdisciplinary applications. The ecological interpretation of OWTs enables tracking of long-term

trends and ecosystem-use changes, river runoff variability, and marine waters intrusion. It provides a tool to detect and assess the effect of prolonged droughts periods, as well as intense storm surges, expected to become more frequent and intense under future climate scenarios. This methodology may also be useful for detecting sewage discharges or studying shifts in aquatic fauna abundance and composition in relation to changes in water types. Beyond academic applications, OWT maps can support environmental monitoring programmes. For example, the European Water Framework Directive (WFD) requires spatial salinity classification to assess the ecological status in transitional waters, defining oligohaline (<5 PSU), mesohaline (5–25 PSU), and polyhaline (<30 PSU) regimes. Fig. 5 shows that significant salinity differences are observed among OWTs, with OWT 15 predominantly reflecting oligohaline conditions, OWTs 11, 13 and 14 mesohaline, and classes 6–9 polyhaline regions. Salinity information from OWT maps can thus be used to delineate boundaries between salinity regimes or detect potential ecological impacts as marine waters intrusion or changes in freshwater regimes.

OWT maps can be used as stand-alone products to aid in identifying pressures (e.g., freshwater inflows), assessing impacts (e.g., changes in turbidity, oxygen levels), identify areas of interest (regarding ecological status) and tracking long-term trends in response to climate or land-use change. Moreover, the integration of OWT data with hydrodynamic and biogeochemical models aligns with the WFD's emphasis on predictive tools for river and estuarine basins management, a current top priority of the EU.

5. Conclusions

This work demonstrated the potential of satellite-derived OWT classification with linked ecological profiles as a powerful and scalable tool for synoptic observation of dynamic estuarine systems under different environmental conditions. Key findings include:

- Identification of ecologically-meaningful OWT proxies: specific OWT classes were identified as indicators for key estuarine processes, such as marine waters intrusion and phytoplankton-dominated waters (OWT 3 and 7) and riverine input (OWTs 11, 13, 15).
- Environmental drivers of OWT variability: distinct OWT patterns were associated with tidal phases, and PCA analysis revealed which classes substitute the dominant OWT under specific environmental forcings.
- Temporal trends and interannual variability: the time-series of OWTs showed seasonal patterns and an increasing interannual trend in frequency of marine waters inside the estuary.

These findings support the use of ecologically-contextualized OWT classification as a practical and informative tool for estuarine monitoring, with clear potential applications in science, management, and policy.

CRediT authorship contribution statement

Giulia Sent: Writing – review & editing, Methodology, Investigation, Formal analysis, Data curation, Conceptualization. **Evangelos Spyrakos:** Writing – review & editing, Supervision, Investigation, Formal analysis. **Thomas Jackson:** Writing – review & editing, Supervision, Methodology. **Elizabeth C. Atwood:** Writing – review & editing, Resources, Methodology, Data curation. **Vanda Brotas:** Writing – review & editing, Resources, Funding acquisition. **Steve Groom:** Writing – review & editing, Resources, Project administration, Funding acquisition. **Ana C. Brito:** Writing – review & editing, Supervision, Funding acquisition, Formal analysis.

Declaration of competing interest

The authors declare that they have no known competing financial interests or personal relationships that could have appeared to influence the work reported in this paper.

Acknowledgments

This work was supported by FCT – Fundação para a Ciência e a Tecnologia, I.P. by project reference and DOI identifier Doi: 10.54499/PRT/BD/153089/2021, and through the project UID/04292/2025. This research was partially funded by the European Commission through the EU Horizon-2020 project CERTO (Copernicus Evolution – Research for harmonised and Transitional water Observation), grant number 870349 through the EC Horizon Europe research and innovation programme project DANUBE4all under grant agreement no. 101093985 and by the CoastNet Research Infrastructure (http://coastnet.pt, PINFRA/22128/2016, *MAR-016.9.1-FEAMPA-00010 and LISBOA2030-FEDER-01319200)*. The authors wish to acknowledge the support of the wider CERTO consortium, who were essential to the completion of this study.

Appendix A. Supplementary data

Supplementary data to this article can be found online at https://doi.org/10.1016/j.jag.2025.104880.

Data availability

Data will be made available on request.

References

Adjovu, G., Stephen, H., James, D., Ahmad, S., 2023. Overview of the application of remote sensing in effective monitoring of water quality parameters. Remote Sens. 15 (7), 1938. https://doi.org/10.3390/rs15071938.

Antunes, C., 2007. Previsão de Marés Portos principais de Portugal. FCUL Webpages. https://webpages.ciencias.ulisboa.pt/~cmantunes/hidrografia/hidro_mares.html (accessed 14 April 2025).

APA, (Agência Portuguesa do Ambiente), 2016. In: Plano de Gestão da Região Hidrográfica do Tejo e Ribeiras do Oeste (RH5), Parte 2 – Caracterização e Diagnóstico. Agência Portuguesa do Ambiente, Lisboa, p. 176.

Arena, M., Pratolongo, P., Loisel, H., Tran, M., Jorge, D., Delgado, A., 2024. Optical water characterization and atmospheric correction assessment of estuarine and coastal waters around the AERONET-OC Bahia Blanca. Front. Remote Sens. 5. https://doi.org/10.3389/frsen.2024.1305787.

Atwood, E.C., Jackson, T., Laurenson, A., Jönsson, B.F., Spyrakos, E., Jiang, D., Sent, G., Selmes, N., Simis, S., Danne, O., Tyler, A., Groom, S., 2024. Framework for regional to global extension of optical water types for remote sensing of optically complex transitional water bodies. Remote Sens. 16 (17), 3267. https://doi.org/10.3390/rs16173267.

Barbier, E., Hacker, S., Kennedy, C., Koch, E., Stier, A., Silliman, B., 2011. The value of estuarine and coastal ecosystem services. Ecol. Monogr. 81, 169–193. https://doi.org/10.1890/10-1510.1.

Bi, S., Hieronymi, M., 2024. Holistic optical water type classification for ocean, coastal, and inland waters. Limnol. Oceanogr. 69 (7), 1547–1561. https://doi.org/10.1002/lno.12606.

Cereja, R., Brotas, V., Nunes, S., Rodrigues, M., Cruz, J.P.C., Brito, A.C., 2022. Tidal influence on water quality indicators in a temperate mesotidal estuary (Tagus Estuary, Portugal). Ecol. Ind. 136. https://doi.org/10.1016/j.ecolind.2022.108715.

De Pablo, H., Sobrinho, J., Garaboa-Paz, D., Fonteles, C., Neves, R., Gaspar, M.B., 2022. The influence of the river discharge on residence time, exposure time and integrated water fractions for the Tagus estuary (Portugal). Front. Mar. Sci. 8, 734814. https://doi.org/10.3389/fmars.2021.734814.

Devred, E., Sathyendranath, S., Platt, T., 2007. Delineation of ecological provinces using ocean colour radiometry. Mar. Ecol. Progr. Series 346. https://doi.org/10.3354/meps07149.

Eleveld, M.A., van der Wal, D., van Kessel, T., 2014. Estuarine suspended particulate matter concentrations from sun-synchronous satellite remote sensing: tidal and meteorological effects and biases. Sens. Environ. Remote. https://doi.org/10.1016/j.rse.2013.12.019.

Eleveld, M.A., Ruescas, A.B., Hommersom, A., Moore, T.S., Peters, S.W.M., Brockmann, C., 2017. An optical classification tool for global lake waters. Remote. Sens. 9 (5), 1–24. https://doi.org/10.3390/rs9050420.

Esper, J., Torbenson, M., Büntgen, U., 2024. Summer warmth unparalleled over the past 2,000 years. Nature 631, 94–97. https://doi.org/10.1038/s41586-024-07512-y.

Fortunato, A.B., Oliveira, A., Baptista, M., 1999. On the effect of tidal flats on the hydrodynamics of the Tagus estuary. Oceanol. Acta 22 (1), 31–44. https://doi.org/10.1016/S0399-1784(99)80030-9.

Fowler, H.J., Blenkinsop, S., Green, A., Devis, P.A., 2024. Precipitation extremes in 2023. Nat. Rev. Earth Environ. 5, 250–252. https://doi.org/10.1038/s43017-024-00547-9.

Gameiro, C., Cartaxana, P., Brotas, V., 2007. Environmental drivers of phytoplankton distribution and composition in Tagus estuary. Estuar. Coast. Shelf Sci. 75 (1/2), 21–34. https://doi.org/10.1016/j.ecss.2007.05.014.

Gameiro, C., Brotas, V., 2010. Patterns of Phytoplankton variability in the Tagus estuary (Portugal). Estuar. Coasts. 33 (2). https://doi.org/10.1007/s12237-009-9194-4.

Gameiro, C., Zwolinski, J., Brotas, V., 2011. Light control on phytoplankton production in a shallow and turbid estuarine system. Hydrobiologia 669 (1), 249–263. https://doi.org/10.1007/s10750-011-0695-3.

Guerreiro, M., Fortunato, A.B., Freire, P., Rilo, A., Taborda, R., Freitas, M.C., Andrade, C., Silva, T., Rodrigues, M., Bertin, X., Azevedo, A., 2015. Evolution of the hydrodynamics of the Tagus estuary (Portugal) in the 21st century. J. Integr. Coast. Zone Manag. 15 (1). https://doi.org/10.5894/rgci515.

Jackson, T., Sathyendranath, S., Mélin, F., 2017. An improved optical classification scheme for the Ocean Colour Essential Climate Variable and its applications. Remote. Sens. of Environ. 203, 152–161. https://doi.org/10.1016/j.rse.2017.03.036.

Moore, T., Dowell, M., Bradt, S., Verdú, A., 2014. An optical water type framework for selecting and blending retrievals from bio-optical algorithms in lakes and coastal waters. Remote. Sens. Environ. 143, 97–111. https://doi.org/10.1016/J.RSE.2013.11.021.

Neves, F., 2010. Dynamics and Hydrology of the Tagus Estuary: Results From in Situ Observations Ph.D. thesis. Available online at: http://repositorio.ul.pt/handle/10451/2003.

Platt, T., Sathyendranath, S., 1999. Spatial structure of pelagic ecosystem processes in the global ocean. Ecosystems 2 (5). https://doi.org/10.1007/s100219900088.

Rodrigues, M., Fortunato, A.B., Freire, P., 2019. Saltwater intrusion in the upper Tagus estuary during droughts. Geosci. (Switzerland) 9 (9). https://doi.org/10.3390/geosciences9090400.

Rodrigues, M., Cravo, A., Freire, P., Rosa, A., Santos, D., 2020. Temporal assessment of the water quality along an urban estuary (Tagus estuary, Portugal). Mar. Chem. 223. https://doi.org/10.1016/j.marchem.2020.103824.

Sent, G., Antunes, G., Spyrakos, E., Jackson, T., C. Atwood, E., Brito A.C., 2025. What time is the tide? The importance of tides for ocean colour applications to estuaries. Remote. Sens. Appl.: Soc. Environ. (37), 101425. Doi: 10.1016/j.rsase.2024.101425.

Stelzer, K., et al., 2020. Copernicus Global Land Operations 'Cryosphere and Water' 'CGLOPS-2 – Lot 2'.

Spyrakos, E., O'Donnell, R., Hunter, P.D., Miller, C., Scott, M., Simis, S.G.H., Neil, C., Barbosa, C.C.F., Binding, C.E., Bradt, S., Bresciani, M., Dall'Olmo, G., Giardino, C., Gitelson, A.A., Kutser, T., Li, L., Matsushita, B., Martinez-Vicente, V., Matthews, M. W., Tyler, A.N., 2018. Optical types of inland and coastal waters. Limnol. Oceanogr. 63 (2), 846–870. https://doi.org/10.1002/lno.10674.

Steinmetz, F., Deschamps, P.Y., Ramon, D., 2011. Atmospheric Correction in Presence of Sunglint: Application to MERIS. Opt. Express 19, 9783. https://doi.org/10.1364/oe.19.009783.

Sun, D., Hu, C., Qiu, Z., Cannizzaro, J., Barnes, B., 2014. Influence of a red band-based water classification approach on chlorophyll algorithms for optically complex estuaries. Remote. Sens. of Environ. 155, 289–302. https://doi.org/10.1016/J.RSE.2014.08.035.

Uudeberg, K., Ansko, I., Põru, G., Ansper, A., Reinart, A., 2019. Using optical water types to monitor changes in optically complex inland and coastal waters. Remote. Sens. 11, 2297. https://doi.org/10.3390/rs11192297.

Uudeberg, K., Aavaste, A., Kõks, K., Ansper, A., Uusõue, M., Kangro, K., Ansko, I., Ligi, M., Toming, K., Reinart, A., 2020. Optical water type guided approach to estimate optical water quality parameters. Remote. Sens. 12, 931. https://doi.org/10.3390/rs12060931.

Vale, C., Sundby, B., 1987. Suspended sediment fluctuations in the Tagus estuary on semi-diurnal and fortnightly time scales. Estuar. Coast. Shelf Sci. https://doi.org/10.1016/0272-7714(87)90110-7.

Valente, A.S., da Silva, J.C.B., 2009. On the observability of the fortnightly cycle of the Tagus estuary turbid plume using MODIS ocean colour images. J. Mar. Syst. https://doi.org/10.1016/j.jmarsys.2008.08.008.

Vaz, N., Dias, J.M., 2014. Residual currents and transport pathways in the Tagus estuary, Portugal: the role of freshwater discharge and wind. J. Coast. Res. 70. https://doi.org/10.2112/SI70-103.1.

Virtanen, P., Gommers, R., Oliphant, T.E., Haberland, M., Reddy, T., Cournapeau, D., Burovski, E., Peterson, P., Weckesser, W., Bright, J., van der Walt, S.J., Brett, M., Wilson, J., Millman, K.J., Mayorov, N., Nelson, A.R.J., Jones, E., Kern, R., Larson, E., Vázquez-Baeza, Y., 2020. SciPy 1.0: fundamental algorithms for scientific computing in Python. Nat. Methods 17 (3). https://doi.org/10.1038/s41592-019-0686-2.

Wei, J., Wang, M., Mikelsons, K., Jiang, L., Kratzer, S., Lee, Z., Moore, T., Sosik, H.M., van der Zande, D., 2022. Global satellite water classification data products over oceanic, coastal, and inland waters. Remote. Sens. Environ. 282. https://doi.org/10.1016/j.rse.2022.113233.

Werdell, P.J., McKinna, L.I.W., Boss, E., Ackleson, S.G., Craig, S.E., Gregg, W.W., Lee, Z., Maritorena, S., Roesler, C.S., Rousseaux, C.S., Stramski, D., Sullivan, J.M., Twardowski, M.S., Tzortziou, M., Zhang, X., 2018. An overview of approaches and challenges for retrieving marine inherent optical properties from ocean color remote sensing. Prog. Oceanogr. 160, 186–212. https://doi.org/10.1016/j.pocean.2018.01.001.

Wevers, J., Müller, D., Scholze, J., Kirches, G., Quast, R., Brockmann, C., 2021. IdePix for Sentinel-2 MSI Algorithm Theoretical Basis Document. Zenodo. https://doi.org/10.5281/zenodo.5788066.

Windle, A.E., Malkin, S.Y., Hood, R.R., Silsbe, G.M., 2025. Optical water typing in optically complex waters: a case study of Chesapeake Bay. Sci. Tot. Env. 981, 179558. https://doi.org/10.1016/j.scitotenv.2025.179558.

Xie, S.P., Miyamoto, A., Zhang, P., Kosaka, Y., Liang, Y., Lutsko, N.J., 2025. What made 2023 and 2024 the hottest years in a row? NPJ Clim. Atmos. Sci. 8, 117. https://doi.org/10.1038/s41612-025-01006-y.

Yue, Y., Qing, S., Diao, R., Hao, Y., 2020. Remote sensing of suspended particulate matter in optically complex estuarine and inland waters based on optical classification. J. Coast. Res. 102, 303–317. https://doi.org/10.2112/SI102-037.1.